



Published in final edited form as:

Circ Res. 2012 May 25; 110(11): 1474–1483. doi:10.1161/CIRCRESAHA.112.268094.

Role of RyR2 Phosphorylation at S2814 during Heart Failure Progression

Jonathan L. Respress^{1,*}, Ralph J. van Oort^{1,*}, Na Li¹, Natale Rolim³, Sayali Dixit¹, Angela deAlmeida¹, Niels Voigt⁴, William S. Lawrence¹, Darlene G. Skapura¹, Kristine Skårdal³, Ulrik Wisloff³, Thomas Wieland⁵, Xun Ai⁶, Steven M. Pogwizd⁶, Dobromir Dobrev⁴, and Xander H.T. Wehrens^{1,2}

¹Department of Molecular Physiology and Biophysics, Baylor College of Medicine, Houston, TX, USA

²Department of Medicine, Baylor College of Medicine, Houston, TX, USA

³K.G. Jebsen Center of Exercise in Medicine, Department of Circulation and Medical Imaging, Faculty of Medicine, Norwegian University of Science and Technology, Trondheim, Norway

⁴Division of Experimental Cardiology, Medical Faculty Mannheim, Heidelberg University, Mannheim, Germany

⁵Institute of Experimental and Clinical Pharmacology and Toxicology, Medical Faculty Mannheim, Heidelberg University, Mannheim, Germany

⁶Department of Medicine, University of Alabama at Birmingham, Birmingham, AL

Abstract

Rationale—Increased activity of Ca²⁺/calmodulin-dependent protein kinase II (CaMKII) is thought to promote heart failure progression. However, the importance of CaMKII phosphorylation of ryanodine receptors (RyR2) in heart failure (HF) development and associated diastolic sarcoplasmic reticulum (SR) Ca²⁺ leak is unclear.

Objective—Determine the role of CaMKII phosphorylation of RyR2 in patients and mice with non-ischemic and ischemic forms of HF.

Methods and Results—Phosphorylation of the primary CaMKII site S2814 on RyR2 was increased in patients with non-ischemic but not with ischemic HF. Knock-in mice with an inactivated S2814 phosphorylation site were relatively protected from HF development following transverse aortic constriction (TAC) compared to wildtype (WT) littermates. After TAC, S2814A mice did not exhibit pulmonary congestion and had reduced levels of atrial natriuretic factor (ANF). Cardiomyocytes from S2814A mice exhibited significantly lower SR Ca²⁺ leak and improved SR Ca²⁺ loading compared to WT mice after TAC. Interestingly, these protective effects on cardiac contractility were not observed in S2814A mice following experimental myocardial infarction.

Conclusions—Our results suggest that increased CaMKII phosphorylation of RyR2 plays a role in the development of pathological SR Ca²⁺ leak and heart failure development in non-ischemic forms of HF such as transverse aortic constriction in mice.

Address correspondence to: Xander H.T. Wehrens, MD, PhD, Baylor College of Medicine, One Baylor Plaza, BCM335, Houston, TX 77030, United States, Tel: 713-798-4261; Fax: 713-798-3475, wehrens@bcm.edu.

*These authors contributed equally to this work.

DISCLOSURES

None.

Keywords

Calcium; CaMKII; heart failure; ryanodine receptor; sarcoplasmic reticulum

INTRODUCTION

Heart failure (HF) is a leading cause of morbidity and mortality and is responsible for 1 of every 9 deaths in the United States alone ¹. Recent studies have revealed that increased activity of the enzyme Ca²⁺/calmodulin-dependent protein kinase II (CaMKII) plays a major role in the development of heart failure ²⁻⁴. CaMKII can promote pathological cardiac remodeling by increasing cell death ⁵, stimulating cardiac dilatation ³, promoting cardiac arrhythmias ⁶, and interfering with excitation-contraction coupling ².

Excitation-contraction coupling is initiated by the influx of extracellular Ca²⁺ via voltage-gated Ca²⁺ channels, which triggers a much greater release of Ca²⁺ from the sarcoplasmic reticulum (SR) ⁷. In the normal heart, the amplitude of SR Ca²⁺ release can be dynamically increased by activation of CaMKII at faster heart rates, leading to a frequency-dependent enhancement of cardiac contractility ⁸. In contrast, it has also been suggested that chronic elevation of CaMKII activity in diseased hearts can cause diastolic Ca²⁺ leak from the SR associated with a loss of contractility ^{6,9}. However, it remains unclear which Ca²⁺ handling proteins downstream of CaMKII are responsible for SR Ca²⁺-release abnormalities, although the ryanodine receptor (RyR2) and phospholamban (PLN) can be functionally altered by CaMKII ^{10,11}.

In previous work, we have demonstrated that CaMKII predominantly regulates RyR2 by phosphorylation of residue S2814 ^{6,8}. This site is near but distinct from the primary PKA phosphorylation site S2808, which also modulates gating properties of the channel ¹². We recently demonstrated that CaMKII phosphorylation of RyR2 is sufficient to increase SR Ca²⁺ leak in mice with constitutively phosphorylated RyR2 due to mutation S2814D ⁶. Moreover, this RyR2-mediated SR Ca²⁺ leak leads to the development of late onset cardiomyopathy in S2814D mice, suggesting that chronic phosphorylation of S2814 might promote the development of heart failure ⁶. These data are consistent with studies showing that pharmacologic or genetic inhibition of CaMKII can prevent or delay the onset of heart failure in animal models ^{4,13}. On the other hand, it has also been shown that PKA hyperphosphorylation of RyR2 at S2808 occurs in failing hearts and that genetic inhibition of S2808 phosphorylation prevents development of ischemic heart failure in some mouse models ^{14,15}. Therefore, the contribution of these two phosphorylation sites on RyR2 in the development of heart failure remains controversial.

Our studies revealed increased phosphorylation of S2814 on RyR2 in patients with non-ischemic dilated cardiomyopathy (DCM) but not in patients with ischemic cardiomyopathy (ICM). Knock-in mice with a genetically inactivated S2814 phosphorylation site (S2814A mutation) were relatively protected from HF development following transverse aortic constriction compared (TAC) to wildtype (WT) littermates. These effects were associated with a decline in the amount of spontaneous SR Ca²⁺ release events following TAC in S2814A mice, attributable to prevention of enhanced S2814 phosphorylation. Interestingly, S2814A mice were not protected from the development of ischemic heart failure following myocardial infarction (MI), consistent with our data obtained in ICM human samples. Thus, our findings suggest that increased CaMKII phosphorylation of RyR2 plays a critical role in the development of pathological SR Ca²⁺ leak and heart failure progression in non-ischemic forms of HF in both humans and transverse aortic constricted mice.

MATERIALS AND METHODS

An expanded Methods section is available in the Online Data Supplement at <http://circres.ahajournals.org> and provides expanded details for surgical procedures, echocardiography, MRI, hemodynamic measurements, histology, Western blot analysis, quantitative RT-PCR, and calcium imaging.

Surgical procedures

Generation of RyR2-S2814A knock-in mice has been described¹⁶. All animal studies were performed according to protocols approved by the Institutional Animal Care and Use Committee of Baylor College of Medicine, conforming to the Guide for the Care and Use of Laboratory Animals published by the US National Institutes of Health (NIH Publication No. 85-23, revised 1996). Transverse aortic constriction (TAC) and myocardial infarction were performed as described^{15, 17}.

Statistical Analysis

All data are represented as average \pm SEM. Statistical significance of differences between experimental groups was determined using Student paired t-test or ANOVA followed by Tukey's post-test when appropriate. A value of $P < 0.05$ was considered statistically significant.

RESULTS

Increased S2814 phosphorylation of RyR2 in patients with non-ischemic dilated cardiomyopathy

Increased activity of CaMKII has been suggested to contribute to contractile dysfunction and hypertrophy development associated with heart failure in patients and animal models^{2, 3, 18}. To determine whether RyR2 phosphorylation by CaMKII is altered in patients with heart failure, we measured RyR2 phosphorylation levels of S2814 (the principal CaMKII site) as well as S2808 (the principal PKA site and potential secondary CaMKII site) using phospho-epitope specific antibodies. Ponceau staining confirmed that similar amounts of heart lysate were loaded on the protein gels. Western blots revealed a significant increase in S2814 phosphorylation in non-ischemic DCM but not in ICM patients, compared with healthy controls (Figure 1). In contrast, there were no significant changes in S2808 phosphorylation of RyR2 in both patient groups. The finding that S2814 phosphorylation of RyR2 is elevated in patients with DCM was confirmed in a second cohort of non-ischemic DCM patients (Online Figure I A–B, and Online Table I). In these samples, increased RyR2 phosphorylation of S2814 may be attributed to enhanced CaMKII activity, since CaMKII T286-autophosphorylation was increased in non-ischemic DCM patients compared to controls (Online Figure I C–D).

S2814A knock-in mice exhibit reduced heart failure development in response to pressure overload

Since previous studies have suggested that CaMKII activity plays an important role in development of heart failure following pressure overload in mice^{13, 18}, we tested whether CaMKII mediated phosphorylation of RyR2 is important for HF development. We studied RyR2-S2814A knock-in mice (S2814A) in which the CaMKII phosphorylation site was genetically inactivated. At baseline, cardiac dimensions and function in S2814A mice were similar to WT mice up to at least 12 months of age, as determined by echocardiography (Online Table II). Next, ten-to-twelve week old S2814A mice (n=9) and WT littermates (n=13) were subjected to TAC. TAC was performed by partial constriction of the transverse aorta between the right and left carotid arteries, which led to pressure overload. Additional

S2814A (n=9) and WT (n=8) mice were subjected to a sham procedure. One-week post-TAC, Doppler ultrasound was performed to measure flow velocity in the right and left carotid arteries to estimate the severity of aortic stenosis¹⁹. The ratio between right and left carotid flow velocities was similar in S2814A (6.9±0.3) and WT mice (6.2±0.2), which indicates that both groups were subjected to similar levels of pressure overload. To determine the effects of the S2814A mutation on development of cardiac hypertrophy and failure, cardiac geometry and function were evaluated using serial echocardiography 0, 4, 8, 12, and 16 weeks following TAC (Figure 2A–C and Table 1).

Echocardiographic analysis revealed a similar hypertrophic response in S2814A and WT mice following TAC evidenced by a similar initial increase in left ventricular posterior wall thickness during diastole (LVPWd) compared to sham mice (Figure 2A). There was, however, a trend towards a lower LVPWd at 16 weeks post-TAC in WT mice compared to S2814A mice (0.78±0.02 mm vs. 0.83±0.04 mm, respectively; *P*=0.20), suggesting ventricular wall thinning as a possible result of cardiac dilation. Indeed, WT mice developed a more pronounced cardiac dilatation following pressure overload in comparison to S2814A mice starting at 12 weeks after surgery (Figure 2B). The ejection fraction (EF) declined similarly in S2814A and WT mice up to 8 weeks after TAC (Figure 2C). However, subsequently only WT mice exhibited a further decline in EF consistent with development of severe heart failure, whereas EF leveled off in S2814A mice. At 16 weeks after TAC, EF was significantly higher in S2814A mice (43.0±2.9%) compared to WT mice (32.4±3.4%, *P*<0.05) (see also Table 1).

To confirm these results, at 16 weeks post-TAC, cardiac contractility was also evaluated using left ventricular (LV) catheterization and pressure-volume measurements (Figure 2D, Online Table III)^{20, 21}. These hemodynamic measurements revealed a significant decrease in the first derivative of LV pressure over time (dP/dt_{max}) in WT mice after TAC (6142 ± 655 mmHg/s) compared with WT sham mice (10498 ± 537 mmHg/s, *P*<0.001), indicating loss of systolic function due to pressure overload (Figure 2E). In S2814A mice, however, dP/dt_{max} was not significantly decreased following TAC (8068 ± 506 mmHg/s) compared to sham (8883 ± 446 mmHg/s). Quantification of diastolic blood pressure (P_{min}, or end-diastolic pressure (EDP)) revealed impaired diastolic function in WT mice after TAC (8.46 ± 3.40 mmHg), which was not seen in S2814A TAC mice (2.08 ± 1.1 mmHg; *P*<0.01; Figure 2F). Thus, these data suggest that inhibition of RyR2 phosphorylation by CaMKII is sufficient to reduce the development of heart failure and preserve cardiac function in a mouse model of non-ischemic heart failure.

Reduction in cardiac dilatation in S2814 mice following TAC

To further study structural changes in the heart induced by TAC, we performed post-mortem analyses of the hearts at 16 weeks post-surgery. Heart weight (HW) to tibia length (TL) ratios were increased in WT mice (13.8±1.4 mg/mm) at 16 weeks post-TAC compared to sham-operated WT mice (7.9±0.4 mg/mm; *P*<0.01; Figure 3A). In contrast, there was a smaller but still significant increase in HW/TL ratios S2814A mice following TAC (9.9±0.6 mg/mm) compared to sham hearts (7.6 ± 0.5 mg/mm; *P*<0.01). In addition, the HW/TL ratio was smaller in S2814A compared to WT mice following TAC (Figure 3A). Hematoxylin and eosin (H&E) staining of transverse cardiac sections confirmed that S2814A mice exhibited a hypertrophic response (i.e., thickening of left ventricular posterior wall) 16 weeks after TAC (Figure 3B). In contrast, WT mice exhibited slightly thinner posterior walls with enlarged cavities (Figure 3C), consistent with cardiac dilatation. Indeed, only hearts from WT mice but not S2814A mice exhibited a significant increase in cardiac anteroposterior diameter at 16 weeks post-TAC (Figure 3D), consistent with our echocardiography data (see Figure 2A–C). Moreover, peak systolic ventricular pressure (P_{max}, mmHg) was decreased in WT mice (121.1±11.5) compared to S2814A mice

(148.7 ± 8.1) following 16 weeks TAC, consistent with more severe HF development in WT mice after TAC. Correlation of Pmax values with HW/TL ratios revealed less cardiac enlargement despite higher pressures in S2814A mice after TAC, consistent with a protective effect of the S2814A mutation (Online Figure II). Therefore, inhibition of CaMKII mediated phosphorylation of RyR2 does not prevent the hypertrophic response, but prevents the progression from hypertrophy to cardiac dilatation and failure in the setting of pressure overload.

Reduced cardiac remodeling associated with heart failure following TAC in S2814A mice

To determine whether genetic inhibition of CaMKII phosphorylation of RyR2 prevented adverse remodeling of the heart following TAC, Masson's trichrome (MT) staining of cardiac sections was performed to measure cardiac fibrosis (Figure 4A–B). Whereas there was a significant increase in the development of cardiac fibrosis in WT mice following TAC, the amount of fibrosis was reduced in S2814A mice post-TAC (Figure 4B). Additionally, WT mice developed a significant increase in lung weight-to-tibia length (LuW/TL) ratio following TAC (14.6 ± 1.7 mg/mm) compared to sham-operated mice (9.5 ± 0.4 mg/mm; $P < 0.05$), which is indicative of pulmonary edema in the context of congestive HF (Figure 4C). In contrast, there was no significant increase in LuW/TL ratio following TAC in S2814A mice (9.4 ± 0.3 mg/mm) compared to sham-operated S2814A mice (9.9 ± 0.6 mg/mm). However, at 16 weeks post-TAC, there was a significant increase in LuW/TL ratio in WT compared to S2814A mice, suggesting a rescue from pulmonary edema development in S2814A mice (Figure 4C).

Another major determinant of stress-induced cardiac remodeling is reactivation of fetal cardiac genes. Therefore, mRNA levels of fetal genes *nppa* (ANF) and *nppb* (BNP) were determined using quantitative PCR. In sham-operated animals, there were no differences in transcript levels comparing S2814A and WT mice. In contrast, TAC induced a significant increase in ANF and BNP levels in WT mice, compared to sham-operated WT mice (Figure 4D–E). On the other hand, there was no increase in ANF levels and a blunted BNP response in S2814A mice compared to WT mice post-TAC. Taken together, these data suggest that inhibition of CaMKII phosphorylation of RyR2 does not suppress the hypertrophic response following pressure overload, but does prevent cellular signs of maladaptive heart failure.

Increased S2814 but not S2808 phosphorylation of RyR2 following TAC

Next, we determined the time course of potential changes in RyR2 phosphorylation at S2814 (the principal CaMKII site) and S2808 (the principal PKA site). Western blotting of ventricular lysates using phosphoepitope-specific antibodies revealed an increase in CaMKII phosphorylation of S2814 on RyR2 in WT mice after TAC (Figure 5A). The level of S2814 phosphorylation displayed a gradual increase, which became significant at 8 and 16 weeks post-TAC (Figure 5B). As expected, there was no phosphorylation of this site in S2814A mice due to the genetic Serine-to-Alanine mutation of this residue. Of note, the observed increase in S2814 phosphorylation in WT mice 8 weeks after TAC coincides with the time point at which WT and S2814A mice start to diverge in terms of cardiac function (see Figure 2C). Global CaMKII activity (assessed by CaMKII T286-autophosphorylation) increased in WT mice after TAC (Online Figure III A–B). However, there was also a trend towards an increase in CaMKII activity in S2814A mice after TAC ($P < 0.16$). Phosphorylation of the S2808 site on RyR2 trended to increase in both S2814A and WT mice in the later stages of HF (Figure 5C–D). In addition, phosphorylation of PLN at site T17 (CaMKII site) increased in WT and S2814A mice (Online Figure III C–D), whereas phosphorylation of PLN at site S16 (PKA site) remained unchanged in TAC groups versus sham controls (Online Figure III E–F).

Inhibition of CaMKII phosphorylation of RyR2 attenuates SR Ca²⁺ Leak after TAC

To determine the mechanisms underlying sustained cardiac function in S2814A mice following TAC, we next determined whether inhibition of CaMKII-mediated phosphorylation of RyR2 attenuated spontaneous SR Ca²⁺ release events (SCR) following pressure overload. Ventricular myocytes isolated from mice at 16 weeks post-TAC or sham surgery were loaded with a Ca²⁺ sensitive dye and imaged under an epifluorescence microscope. In previous studies²², we found a good correlation between SR Ca²⁺ leak measured using the tetracaine protocol²³ and the number of spontaneous Ca²⁺ release events (SCR). Following 1 Hz pacing to obtain steady-state, the number of SCR events was measured following termination of pacing over a 40-second time period (Figure 6A). The number of myocytes in which SCR events occurred was significantly higher in WT mice following TAC (46 events in 75 cells (~61%)) compared to WT sham mice (8 events in 31 cells (~26%), $P < 0.01$) (Figure 6B). In addition, SCR amplitude (measured as $\Delta F/F_0$) was also increased in WT TAC compared to WT sham mice. In contrast, SCR amplitude was not increased in S2814A TAC compared to S2814A sham mice (Online Figure IV A). The increase in SCR was not due to increased SR Ca²⁺ loading, since SR content was decreased in WT TAC ($\Delta F/F_0$: 1.54 ± 0.1) compared with WT sham mice (1.97 ± 0.2 ; $P < 0.05$) (Online Figure IV B). Moreover, the increase in SCR amplitude was also not due to increased SR Ca²⁺ content, as each release event was normalized to SR Ca²⁺ content (Online Figure IV C).

There were no differences in the rate of reuptake of Ca²⁺ into the SR, a measure of SERCA activity (τ , τ) (Online Figure IV D). The incidence of SCR in myocytes from S2814A mice post-TAC (29.7%) was not increased compared to sham-operated S2814A mice (29.4%), and was significantly lower than myocytes from WT mice post-TAC (61.3%, $P < 0.01$) (Figure 6B). Moreover, SR Ca²⁺ content remained unchanged in S2814A mice post-TAC (1.88 ± 0.1) and S2814A sham mice (1.96 ± 0.2) (Online Figure IV B). These data suggest that the increase in SCR incidence in WT mice following TAC is due to increased S2814 phosphorylation on RyR2 induced by TAC.

Similar findings were obtained when the average number of SCR was quantified per myocyte (Figure 6C). In WT mice, there was a significant increase in SCR events per myocyte over a 40-second time period following TAC (2.0 ± 0.3 events/cell) in comparison to WT sham (0.4 ± 0.1 ; $P < 0.01$). This increase in SCR event rate attributed to TAC was blunted in S2814A mice (0.4 ± 0.1 ; $P < 0.01$). Finally, addition of the global CaMKII inhibitor KN93 also significantly reduced the SCR incidence and number of SCR events per cell in myocytes from WT mice post-TAC (Figure 6B–C). However, KN93 had no additional effect on SCR incidence or events in S2814A TAC cells, suggesting a specific and major role for S2814 phosphorylation on RyR2 in the development of HF.

Inhibition of S2814 phosphorylation on RyR2 fails to protect against heart failure induced by myocardial infarction

Previous studies demonstrated that PKA phosphorylation of RyR2 played a role in the development of ischemic HF following MI¹⁵, but not following TAC-induced pressure overload²⁴. However, these data are controversial in view of a recent study that argued against a role for PKA phosphorylation of RyR2 following MI²⁵. To determine the functional importance of CaMKII phosphorylation of RyR2 during the development of ischemic HF, we subjected S2814A knock-in and WT mice to left anterior descending coronary artery (LAD) ligation to induce myocardial infarction (MI). In mice subjected to the sham procedure, cardiac dimensions and contractility (Supplemental Table S3) were similar in S2814A mice compared to WT mice. The effects of both mild (30% infarct area) and severe (60% infarct area) MI were determined in two separate experimental groups of

S2814A and WT mice (Figure 7A and B) as determined by MRI and echocardiography, and confirmed by histology. Infarct size did not differ in the '30% group' comparing S2814A ($32.8 \pm 2.2\%$) and WT mice ($32.4 \pm 1.0\%$), nor in the '60% group' comparing S2814A ($61.8 \pm 2.1\%$) and WT ($64.9 \pm 4.0\%$). Echocardiography revealed that there were no differences in the relative increase in left ventricular end-diastolic diameter comparing S2814A and WT mice after both 30% and 60% MI three weeks after surgery (Figure 7A). As expected, cardiac dilatation was more pronounced following 60% infarction compared to 30% infarction. Similarly, there was an equal decline in ejection fraction (EF) in S2814A and WT mice following both 30% and 60% MI (Figure 7B). There were no significant differences in EF comparing S2814A and WT mice. At the end of the experiment, ventricular myocytes were isolated from the sham and 60% MI mice. At three weeks after coronary artery ligation, ventricular myocyte length was increased similarly in S2814A and WT mice (Figure 7C).

To determine the levels of CaMKII-mediated RyR2 phosphorylation in response to MI, we performed Western blot analysis of ventricular lysates obtained from mice subjected to 60% MI. Using phospho-specific antibodies, the level of S2814 phosphorylation on RyR2 was significantly decreased in WT mice post-MI ($P < 0.001$). As expected, there was no phosphorylation of S2814 in S2814A mice due to the genetic mutation of this site (Online Figure V A–B). Taken together, these data suggest that inhibition of CaMKII phosphorylation on S2814 of RyR2 does not prevent the development of HF induced by MI.

DISCUSSION

There is ample evidence that CaMKII plays a role in the development of heart failure. Previous studies demonstrated increased expression and activity levels of CaMKII in animals and patients with congestive heart failure^{10, 26, 27}. Transgenic overexpression of CaMKII- δ causes heart failure in mice³, whereas overexpression of a peptide blocker of CaMKII delays the onset of heart failure in AC3-I transgenic mice⁴. Moreover, knockout of CaMKII- δ was shown to limit the progression to heart failure^{13, 18}. It was shown that CaMKII- δ ablation reduced ventricular dilatation and fibrosis, and enhanced cardiac contractility after TAC¹³. The beneficial effects of CaMKII- δ ablation have been attributed to a reduction of SR Ca²⁺ leak, although the downstream targets of CaMKII responsible for these effects were not identified.

The results of the current study revealed increased CaMKII phosphorylation of RyR2 in patients with non-ischemic DCM but not in patients with ICM. These findings suggest that the level of CaMKII activation might depend on the type of heart failure in patients. Previous studies have clearly demonstrated activation of CaMKII- δ by pressure overload in mice^{13, 18, 28}. Our data in mice showed that S2814 phosphorylation on RyR2 is increased in mice subjected to TAC (pressure overload) but not following MI. An important observation was that S2814 phosphorylation increases over time following TAC in WT mice, whereas ablation of the S2814 site alone provided a beneficial effect on deterioration towards severe heart failure in these mice. Thus, our data now identify RyR2 as a downstream target of CaMKII involved in heart failure following pressure overload.

Moreover, our data in mice subjected to TAC revealed increased CaMKII phosphorylation of PLN at T17, but not at the PKA site S16. These findings suggest that activated CaMKII phosphorylates multiple downstream targets in failing hearts. However, the protective effects of the S2814A mutation in RyR2 in mice subjected to TAC shows that RyR2 is a preminent downstream target of CaMKII in this model of heart failure, associated with detrimental remodeling of the heart. Thus, RyR2 phosphorylation at S2814 plays a role in the progression of cardiac hypertrophy to heart failure following TAC.

Transgenic overexpression of CaMKII- δ induces transient cardiac hypertrophy followed by dilated cardiomyopathy and heart failure in mice³. However, hypertrophic remodeling induced by pressure overload was not attenuated in CaMKII- δ deficient mice, suggesting that CaMKII- δ is not required for the development of cardiac hypertrophy in response to TAC¹³. Our data are in agreement with those prior studies in CaMKII- δ deficient mice, as S2814A mice also developed a hypertrophic remodeling similar to WT mice in the early stages following TAC.

Relative importance of RyR2 phosphorylation sites subsequent to heart failure

There has been considerable controversy about the relative importance of RyR2 phosphorylation sites, in particular the S2808 and S2814 sites^{2, 10, 12, 15}. Our studies demonstrated that CaMKII phosphorylation of S2814 on RyR2 was increased following pressure overload induced by TAC, which correlated to our findings in non-ischemic DCM patients (Figure 1). These data are consistent with recent studies by Ling *et al.*¹³. The fact that genetic ablation of this site only prevented the development of decompensation following TAC confirms the importance of S2814 in the pathogenesis of congestive heart failure induced by TAC. Our data also show that phosphorylation of the PKA site S2808 increases, however not significantly, following chronic TAC during later stages of heart failure development. Those findings are in agreement with a prior study showing that genetic ablation of the S2808 site did not ameliorate the development of heart failure in S2808A knock-in mice following TAC²⁴.

It has been proposed that chronically elevated plasma levels of catecholamines may promote PKA hyperphosphorylation of RyR2 in heart failure and contribute to abnormal SR Ca²⁺ release^{14, 29}. Genetic inhibition of phosphorylation of the main PKA site S2808 was shown to reduce the development of MI-induced heart failure in S2808A knock-in mice¹⁵. In addition, a recent study by Shan *et al.*¹² demonstrated that S2808D knock-in mice with constitutively activated PKA phosphorylation sites on RyR2 developed spontaneous heart failure with age, and also exhibited increased mortality after MI. However, our data did not reveal increased S2808 phosphorylation in patients with non-ischemic DCM or ICM. Moreover, Zhang *et al.*²⁵ recently reported a lack of protective effects in S2808A mice following myocardial infarction, adding to the controversy in the field about the importance of S2808 phosphorylation in heart failure development. Interestingly, this paper did show increased S2808 phosphorylation after MI. One possible explanation for the discrepant findings is that PKA hyperphosphorylation may only occur in advanced, more severe stages of ischemic HF. Unless studies are performed at the same time points or severity of cardiac decompensation, phosphorylation levels of S2808 might greatly vary between studies. In addition, there may be regional differences in ischemic failing hearts.

Although prior studies had implicated activation of CaMKII in heart failure development following MI,^{4, 30} the role of CaMKII phosphorylation of RyR2 at S2814 had not been studied before in sufficient detail. Our data revealed that the level of S2814 phosphorylation on RyR2 slightly decreased following MI. Therefore, it was not surprising that S2814A knock-in mice were not protected from developing decompensated heart failure after MI. These findings are in agreement with recent work by Kushnir *et al.*³¹, who also demonstrated a lack of protection from MI-induced heart failure in S2814A mice.

Effects of CaMKII phosphorylation of RyR2 on SR Ca²⁺ leak in heart failure

Enhanced activity of CaMKII in the heart profoundly affects SR Ca²⁺ handling². Ventricular myocytes isolated from CaMKII- δ c transgenic mice exhibit increased diastolic SR Ca²⁺ release events (SR Ca²⁺ leak) despite a lower SR Ca²⁺ load², which could be in part caused by increased CaMKII phosphorylation of RyR2. Phosphorylation of the CaMKII

phosphorylation site S2814 on RyR2 enhances channel open probability and Ca^{2+} spark activity^{6,8}. Our recent studies revealed that constitutive activation of this CaMKII site in S2814D knock-in mice causes SR Ca^{2+} leak, which is associated with a mild dilated cardiomyopathy at 12 months of age⁶. Moreover, S2814D mice exhibit markedly reduced survival following TAC, suggesting that maximal phosphorylation of S2814 on RyR2 promotes development of decompensated heart failure⁶.

Our data revealed an increased incidence of spontaneous SR Ca^{2+} release (SCR) events in wildtype mice after TAC. Pharmacological inhibition of CaMKII reduced the number of SCR events, suggesting that CaMKII activation following pressure overload underlies Ca^{2+} release defects, as previously shown^{2,13}. Genetic ablation of the S2814 phosphorylation site on RyR2 led to a similar decrease in SCR incidence following TAC in the absence of exogenous CaMKII blockade, suggesting that RyR2 is a major downstream target of CaMKII underlying defective SR Ca^{2+} release. Thus, pressure overload induces spontaneous releases of SR Ca^{2+} during diastole due to increased CaMKII mediated phosphorylation of RyR2. Taken together, these data suggest that the preservation of cardiac contractility, attenuation of SR Ca^{2+} leak, and delayed development of heart failure in S2814A mice is mediated by the direct prevention of CaMKII phosphorylation of site S2814 on the RyR2 Ca^{2+} release channel.

Conclusions

Taken together, our present work has demonstrated that increased CaMKII phosphorylation of S2814 on RyR2 plays a critical role in the development of pathological SR Ca^{2+} leak and heart failure in a mouse model of pressure overload. However, phosphorylation of the S2814 site does not appear to play a role in the development of heart failure following myocardial infarction. Moreover, there seems to be a difference in phosphorylation of RyR2 sites depending on whether heart failure is ischemic in nature or not. Overall, our current findings suggest an important role for CaMKII-mediated phosphorylation of S2814 on RyR2 in the development of non-ischemic heart failure in mice with pressure overload, and supports its role as a potential new target for the treatment of heart failure.

Supplementary Material

Refer to Web version on PubMed Central for supplementary material.

Acknowledgments

SOURCES OF FUNDING

X.H.T.W. is a W.M. Keck Foundation Distinguished Young Scholar in Medical Research, and is also supported by NIH/NHLBI grants R01-HL089598 and R01-R01HL091947, and Muscular Dystrophy Association. J.L.R. is a recipient of the 2010 Ruth L. Kirschstein National Research Service Award (NRSA) supported by NIH/NHLBI grant F31-HL099290-01. R.J.v.O. was a recipient of the American Physiological Society Postdoctoral Fellowship in Physiological Genomics. This work was also supported in part by Fondation Leducq (Alliance for CaMKII Signaling in Heart) to X.H.T.W. and S.M.P., the European North-American Atrial Fibrillation Research Alliance to D.D., and by the German Center for Cardiovascular Research (to D.D. and T.W).

The authors would like to thank Julia Reynolds and Claudia Liebetrau for their expertise and technical assistance.

NON-STANDARD ABBREVIATIONS AND ACRONYMS

ANF	Atrial natriuretic factor
BNP	brain natriuretic peptide

CaMKII	Ca ²⁺ /calmodulin-dependent protein kinase II
DCM	dilated cardiomyopathy
ICM	ischemic cardiomyopathy
MI	myocardial infarction
PKA	protein kinase A
PLN	phospholamban
RyR2	ryanodine receptor type 2
SERCA2a	sarco/endoplasmic reticulum Ca ²⁺ -ATPase 2a
SR	sarcoplasmic reticulum
TAC	transverse aortic constriction
MI	myocardial infarction
HF	heart failure
WT	wildtype
SCR	spontaneous calcium release
LVPWd	left ventricular posterior wall diameter during diastole
EF	ejection fraction
EDD	end-diastolic diameter
Pmin	end-diastolic pressure
Pmax	end-systolic pressure
HW	heart weight
LuW	lung weight
TL	tibia length
PCR	polymerase chain reaction
LAD	left anterior descending coronary artery
MRI	magnetic resonance imaging

References

1. Roger VL, Go AS, Lloyd-Jones DM, Adams RJ, Berry JD, Brown TM, Carnethon MR, Dai S, de Simone G, Ford ES, Fox CS, Fullerton HJ, Gillespie C, Greenlund KJ, Hailpern SM, Heit JA, Ho PM, Howard VJ, Kissela BM, Kittner SJ, Lackland DT, Lichtman JH, Lisabeth LD, Makuc DM, Marcus GM, Marelli A, Matchar DB, McDermott MM, Meigs JB, Moy CS, Mozaffarian D, Mussolino ME, Nichol G, Paynter NP, Rosamond WD, Sorlie PD, Stafford RS, Turan TN, Turner MB, Wong ND, Wylie-Rosett J. Heart disease and stroke statistics--2011 update: a report from the American Heart Association. *Circulation*. 2011; 123:e18–e209. [PubMed: 21160056]
2. Maier LS, Zhang T, Chen L, DeSantiago J, Brown JH, Bers DM. Transgenic CaMKII δ C overexpression uniquely alters cardiac myocyte Ca²⁺ handling: reduced SR Ca²⁺ load and activated SR Ca²⁺ release. *Circ Res*. 2003; 92:904–911. [PubMed: 12676813]
3. Zhang T, Maier LS, Dalton ND, Miyamoto S, Ross J Jr, Bers DM, Brown JH. The δ C isoform of CaMKII is activated in cardiac hypertrophy and induces dilated cardiomyopathy and heart failure. *Circ Res*. 2003; 92:912–919. [PubMed: 12676814]

4. Zhang R, Khoo MS, Wu Y, Yang Y, Grueter CE, Ni G, Price EE Jr, Thiel W, Guatimosim S, Song LS, Madu EC, Shah AN, Vishnivetskaya TA, Atkinson JB, Gurevich VV, Salama G, Lederer WJ, Colbran RJ, Anderson ME. Calmodulin kinase II inhibition protects against structural heart disease. *Nat Med.* 2005; 11:409–417. [PubMed: 15793582]
5. Khoo MS, Li J, Singh MV, Yang Y, Kannankeril P, Wu Y, Grueter CE, Guan X, Oddis CV, Zhang R, Mendes L, Ni G, Madu EC, Yang J, Bass M, Gomez RJ, Wadzinski BE, Olson EN, Colbran RJ, Anderson ME. Death, cardiac dysfunction, and arrhythmias are increased by calmodulin kinase II in calcineurin cardiomyopathy. *Circulation.* 2006; 114:1352–1359. [PubMed: 16982937]
6. van Oort RJ, McCauley MD, Dixit SS, Pereira L, Yang Y, Respress JL, Wang Q, De Almeida AC, Skapura DG, Anderson ME, Bers DM, Wehrens XH. Ryanodine receptor phosphorylation by calcium/calmodulin-dependent protein kinase II promotes life-threatening ventricular arrhythmias in mice with heart failure. *Circulation.* 2010; 122:2669–2679. [PubMed: 21098440]
7. Wehrens XH, Lehnart SE, Marks AR. Intracellular calcium release and cardiac disease. *Annu Rev Physiol.* 2005; 67:69–98. [PubMed: 15709953]
8. Wehrens XH, Lehnart SE, Reiken SR, Marks AR. Ca²⁺/calmodulin-dependent protein kinase II phosphorylation regulates the cardiac ryanodine receptor. *Circ Res.* 2004; 94:e61–70. [PubMed: 15016728]
9. Guo T, Zhang T, Mestral R, Bers DM. Ca²⁺/Calmodulin-dependent protein kinase II phosphorylation of ryanodine receptor does affect calcium sparks in mouse ventricular myocytes. *Circ Res.* 2006; 99:398–406. [PubMed: 16840718]
10. Ai X, Curran JW, Shannon TR, Bers DM, Pogwizd SM. Ca²⁺/calmodulin-dependent protein kinase modulates cardiac ryanodine receptor phosphorylation and sarcoplasmic reticulum Ca²⁺ leak in heart failure. *Circ Res.* 2005; 97:1314–1322. [PubMed: 16269653]
11. Zhang T, Guo T, Mishra S, Dalton ND, Kranias EG, Peterson KL, Bers DM, Brown JH. Phospholamban ablation rescues sarcoplasmic reticulum Ca(2+) handling but exacerbates cardiac dysfunction in CaMKII δ (C) transgenic mice. *Circ Res.* 2010; 106:354–362. [PubMed: 19959778]
12. Shan J, Betzenhauser MJ, Kushnir A, Reiken S, Meli AC, Wronska A, Dura M, Chen BX, Marks AR. Role of chronic ryanodine receptor phosphorylation in heart failure and beta-adrenergic receptor blockade in mice. *J Clin Invest.* 2010; 120:4375–4387. [PubMed: 21099115]
13. Ling H, Zhang T, Pereira L, Means CK, Cheng H, Gu Y, Dalton ND, Peterson KL, Chen J, Bers D, Heller Brown J. Requirement for Ca²⁺/calmodulin-dependent kinase II in the transition from pressure overload-induced cardiac hypertrophy to heart failure in mice. *J Clin Invest.* 2009; 119:1230–1240. [PubMed: 19381018]
14. Marx SO, Reiken S, Hisamatsu Y, Jayaraman T, Burkhoff D, Rosembly N, Marks AR. PKA phosphorylation dissociates FKBP12.6 from the calcium release channel (ryanodine receptor): defective regulation in failing hearts. *Cell.* 2000; 101:365–376. [PubMed: 10830164]
15. Wehrens XH, Lehnart SE, Reiken S, Vest JA, Wronska A, Marks AR. Ryanodine receptor/calcium release channel PKA phosphorylation: a critical mediator of heart failure progression. *Proc Natl Acad Sci U S A.* 2006; 103:511–518. [PubMed: 16407108]
16. Chelu MG, Sarma S, Sood S, Wang S, van Oort RJ, Skapura DG, Li N, Santonastasi M, Muller FU, Schmitz W, Schotten U, Anderson ME, Valderrabano M, Dobrev D, Wehrens XH. Calmodulin kinase II-mediated sarcoplasmic reticulum Ca²⁺ leak promotes atrial fibrillation in mice. *J Clin Invest.* 2009; 119:1940–1951. [PubMed: 19603549]
17. deAlmeida AC, van Oort RJ, Wehrens XH. Transverse aortic constriction in mice. *J Vis Exp.*
18. Backs J, Backs T, Neef S, Kreuzer MM, Lehmann LH, Patrick DM, Grueter CE, Qi X, Richardson JA, Hill JA, Katus HA, Bassel-Duby R, Maier LS, Olson EN. The delta isoform of CaM kinase II is required for pathological cardiac hypertrophy and remodeling after pressure overload. *Proc Natl Acad Sci U S A.* 2009; 106:2342–2347. [PubMed: 19179290]
19. Reddy AK, Taffet GE, Li YH, Lim SW, Pham TT, Pocius JS, Entman ML, Michael LH, Hartley CJ. Pulsed Doppler signal processing for use in mice: applications. *IEEE Trans Biomed Eng.* 2005; 52:1771–1783. [PubMed: 16235663]

20. Kottam AT, Porterfield J, Raghavan K, Fernandez D, Feldman MD, Valvano JW, Pearce JA. Real time pressure-volume loops in mice using complex admittance: measurement and implications. *Conf Proc IEEE Eng Med Biol Soc.* 2006; 1:4336–4339. [PubMed: 17946238]
21. Joho S, Ishizaka S, Sievers R, Foster E, Simpson PC, Grossman W. Left ventricular pressure-volume relationship in conscious mice. *Am J Physiol Heart Circ Physiol.* 2007; 292:H369–377. [PubMed: 16905597]
22. Sarma S, Li N, van Oort RJ, Reynolds C, Skapura DG, Wehrens XH. Genetic inhibition of PKA phosphorylation of RyR2 prevents dystrophic cardiomyopathy. *Proc Natl Acad Sci U S A.* 107:13165–13170. [PubMed: 20615971]
23. Shannon TR, Pogwizd SM, Bers DM. Elevated sarcoplasmic reticulum Ca²⁺ leak in intact ventricular myocytes from rabbits in heart failure. *Circ Res.* 2003; 93:592–594. [PubMed: 12946948]
24. Benkusky NA, Weber CS, Scherman JA, Farrell EF, Hacker TA, John MC, Powers PA, Valdivia HH. Intact beta-adrenergic response and unmodified progression toward heart failure in mice with genetic ablation of a major protein kinase A phosphorylation site in the cardiac ryanodine receptor. *Circ Res.* 2007; 101:819–829. [PubMed: 17717301]
25. Zhang H, Makarewich C, Kubo H, Wang W, Duran J, Li Y, Berretta R, Koch WJ, Chen X, Gao E, Valdivia H, Houser SR. Hyperphosphorylation of the Cardiac Ryanodine Receptor at Serine 2808 Is Not Involved in Cardiac Dysfunction After Myocardial Infarction. *Circ Res.* 2012 In press.
26. Hoch B, Meyer R, Hetzer R, Krause EG, Karczewski P. Identification and expression of delta-isoforms of the multifunctional Ca²⁺/calmodulin-dependent protein kinase in failing and nonfailing human myocardium. *Circ Res.* 1999; 84:713–721. [PubMed: 10189359]
27. Hagemann D, Bohlender J, Hoch B, Krause EG, Karczewski P. Expression of Ca²⁺/calmodulin-dependent protein kinase II delta-subunit isoforms in rats with hypertensive cardiac hypertrophy. *Mol Cell Biochem.* 2001; 220:69–76. [PubMed: 11451385]
28. Colomer JM, Mao L, Rockman HA, Means AR. Pressure overload selectively up-regulates Ca²⁺/calmodulin-dependent protein kinase II in vivo. *Mol Endocrinol.* 2003; 17:183–192. [PubMed: 12554746]
29. Reiken S, Wehrens XH, Vest JA, Barbone A, Klotz S, Mancini D, Burkhoff D, Marks AR. Beta-blockers restore calcium release channel function and improve cardiac muscle performance in human heart failure. *Circulation.* 2003; 107:2459–2466. [PubMed: 12743001]
30. He BJ, Joiner ML, Singh MV, Luczak ED, Swaminathan PD, Koval OM, Kutschke W, Allamargot C, Yang J, Guan X, Zimmerman K, Grumbach IM, Weiss RM, Spitz DR, Sigmund CD, Blankesteyn WM, Heymans S, Mohler PJ, Anderson ME. Oxidation of CaMKII determines the cardiotoxic effects of aldosterone. *Nat Med.* 2011; 17:1610–1618. [PubMed: 22081025]
31. Kushnir A, Shan J, Betzenhauser MJ, Reiken S, Marks AR. Role of CaMKII δ phosphorylation of the cardiac ryanodine receptor in the force frequency relationship and heart failure. *Proc Natl Acad Sci U S A.* 2010; 107:10274–10279. [PubMed: 20479242]

NOVELTY AND SIGNIFICANCE

What is known?

- Heart failure (HF) is a leading cause of morbidity and mortality and is responsible for 1 of every 9 deaths in the United States.
- Ca²⁺/calmodulin-dependent protein kinase II (CaMKII) is upregulated in patients with HF.
- Phosphorylation of CaMKII phosphorylation site S2814 on RyR2 enhances open probability, Ca²⁺ spark activity and sarcoplasmic reticulum (SR) Ca²⁺ leak

What new information does this article contribute?

- S2814 phosphorylation of RyR2 is increased in patients with non-ischemic dilated cardiomyopathy (DCM) and mice following pressure overload, but not in patients and mice with ischemic cardiomyopathy (ICM).
- Genetic inhibition of S2814 phosphorylation of RyR2 prevents SR Ca leak and decompensated HF following transverse aortic constriction (TAC) in mice.

Previous studies demonstrated that increased levels of CaMKII might contribute to enhanced sarcoplasmic reticulum (SR) Ca leak in animals and patients with HF. Here, we tested the hypothesis that CaMKII phosphorylation of S2814 on RyR2 underlies Ca cycling defects in heart failure. First, we found that S2814 phosphorylation is only increased in patients with non-ischemic DCM, but not in those with ICM. Next, genetic inhibition of S2814 phosphorylation in mice was found to prevent development of decompensated HF following TAC. The time course of the protective effect correlated well with the delayed increase in S2814 phosphorylation on RyR2. Finally, SR Ca leak was reduced in S2814A knock-in mice after TAC, compared to WT control mice. In contrast, S2814A mice were not protected from developing HF following myocardial infarction, consistent with the findings in human ICM samples. Thus, our data suggest that increased S2814 phosphorylation of RyR2 might play an important role in development of non-ischemic types of HF.

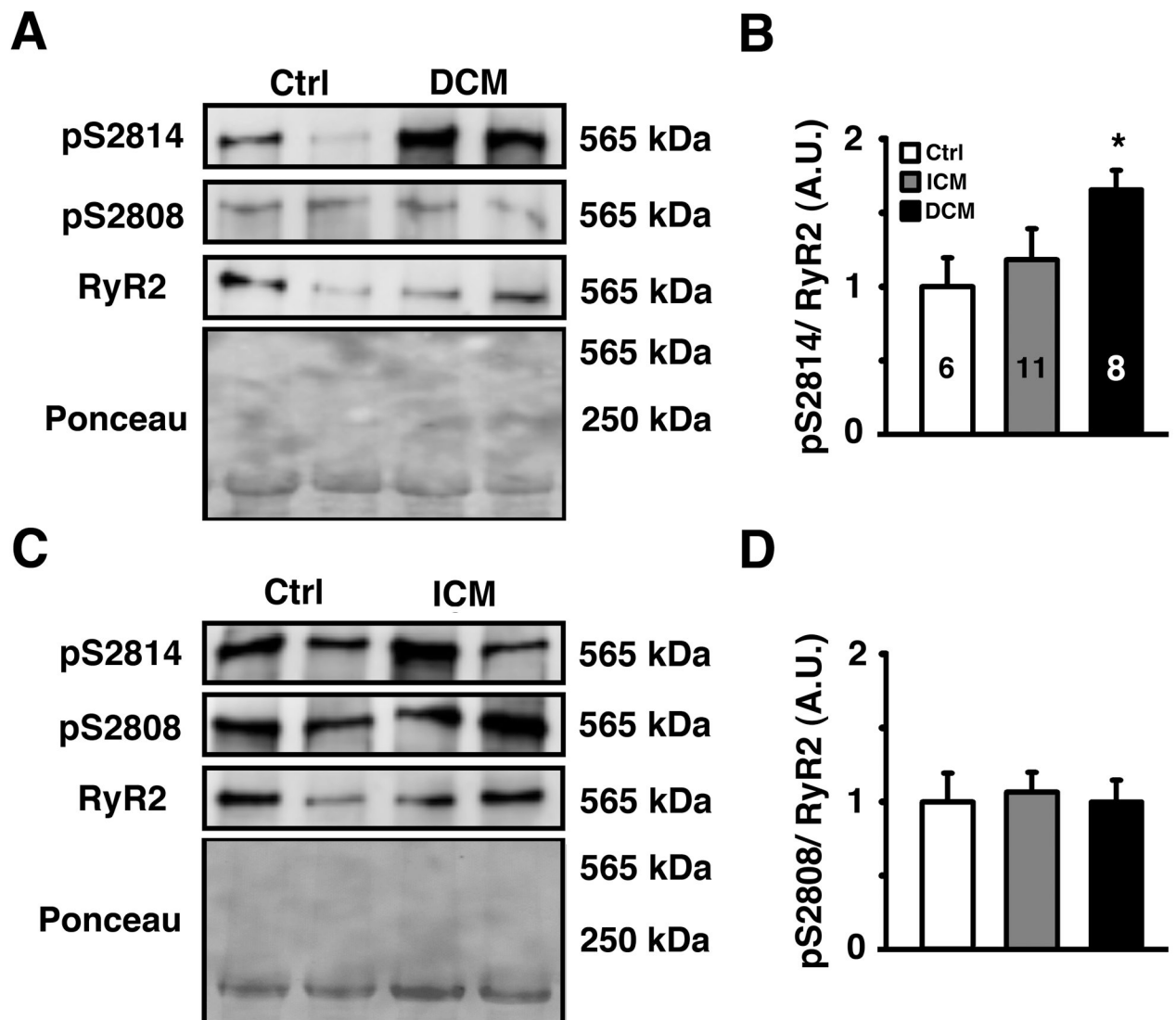


Figure 1. Increased S2814 phosphorylation on RyR2 in patients with non-ischemic DCM
A. Representative Western blots for phosphorylated RyR2-S2814 (pS2814), RyR2-S2808 (pS2808), and total RyR2 in heart lysates from healthy humans and patients with non-ischemic dilated cardiomyopathy (DCM). Total amount of protein was determined by Ponceau staining. **B.** Quantification revealed an increased S2814 phosphorylation in DCM but no change in ICM patients. Numbers in bar indicate number of patients analyzed in panels B and D. **C.** Representative Western blots for phosphorylated RyR2-S2814 (pS2814), RyR2-S2808 (pS2808) and total RyR2 in heart lysates from healthy humans and patients with ischemic cardiomyopathy (ICM). **D.** Quantification revealed no change in S2808 phosphorylation in both patients groups. Data represented as average \pm SEM. * $P < 0.05$ versus corresponding control.

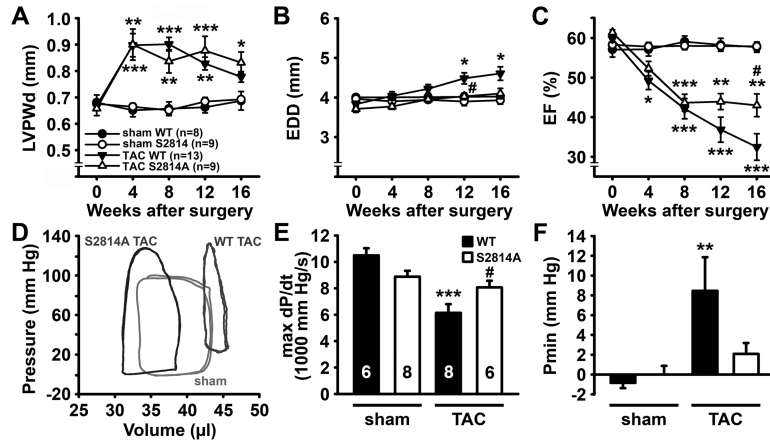


Figure 2. S2814A mice exhibit delayed progression of heart failure following TAC

A–C. Echocardiographic analysis of left ventricular posterior wall diameter (LVPWd) (**A**), end-diastolic diameter (**B**), and ejection fraction (EF) (**C**) in S2814A mice or WT littermates before, 4, 8, 12, and 16 weeks after sham or transverse aortic constriction (TAC), respectively. **D.** Representative pressure-volume loops at 16 weeks post-TAC showing reduced LV diastolic volume and improved contractility in a S2814A mouse compared to WT. Representative loops indicate one animal per group. Numbers in panel A indicate number of animals used in panels A–D. **E.** Bar graph showing significant decrease in cardiac contractility (dP/dt) in WT mice following TAC, which was blunted in S2814A mice. Numbers in bar indicate number of animals used in panels E–F. **F.** Unlike WT mice, S2814A mice did not develop elevated end-diastolic LV pressure at 16 weeks post-TAC. * $P < 0.05$, ** $P < 0.01$, *** $P < 0.001$ versus corresponding sham group, # $P < 0.05$ versus WT TAC.

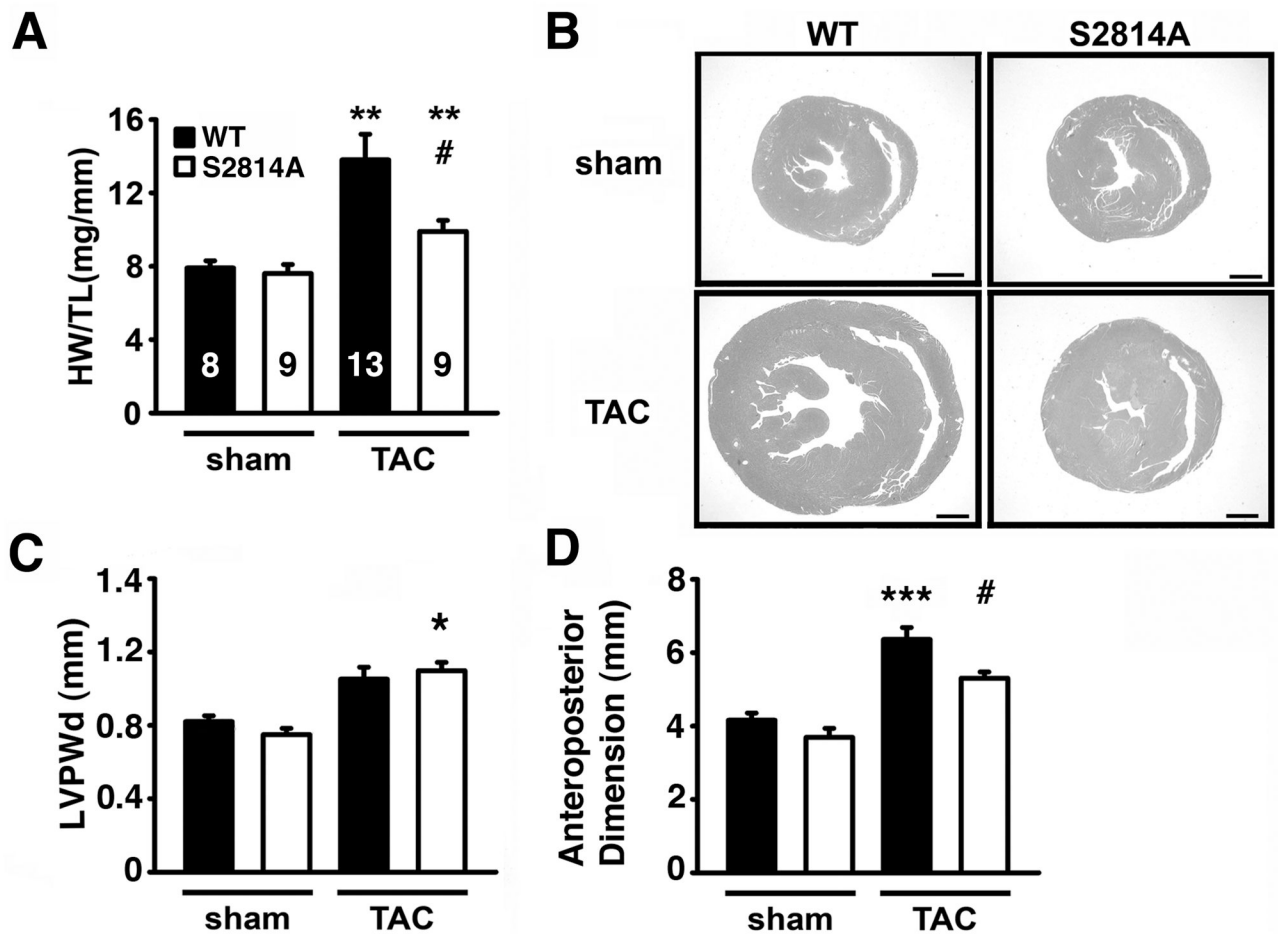


Figure 3. Reduction in cardiac dilatation in S2814 mice following TAC

A. Heart weight-to-tibia length (HW/TL) ratios at 16 weeks after TAC. Numbers in bar indicate number of animals used in panels A–D. **B.** Representative photographs of midsagittal sections stained with H&E showing reduced cardiac enlargement in S2814A mice following TAC. Scale bar, 1 mm. **C, D.** Left ventricular posterior wall thickness (**C**) and anteroposterior left ventricular diameters (**D**) measured in histological sections. * $P < 0.05$, ** $P < 0.01$, *** $P < 0.001$ versus corresponding sham group; # $P < 0.05$ versus WT TAC.

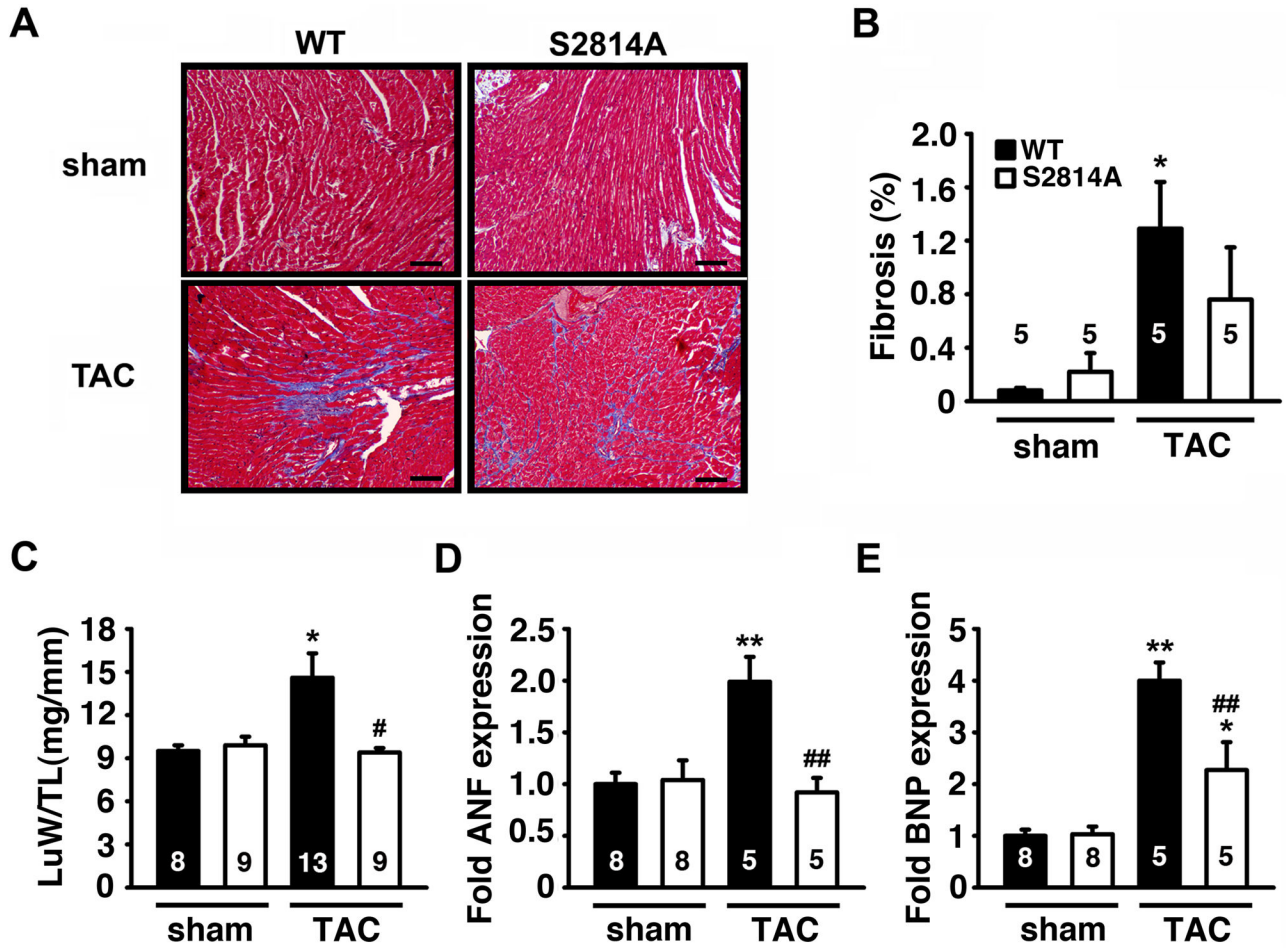


Figure 4. Reduced cardiac remodeling associated with heart failure following TAC in S2814A mice

A. Representative photographs of sections at the midsagittal level of hearts stained with Masson's Trichrome (scale bar = 1 mm). **B.** Quantification of cardiac fibrosis at 16 weeks after sham or TAC surgery. **C.** Post-mortem measurements of lung weight to tibia length (LuW/TL) ratios 16 weeks after TAC. **D, E.** mRNA transcript levels of cardiac stress genes ANF (**D**) and BNP (**E**) by real-time PCR. Numbers in bar indicate number of animals. * $P < 0.05$, ** $P < 0.01$ versus corresponding sham group; # $P < 0.05$, ## $P < 0.01$ versus WT TAC.

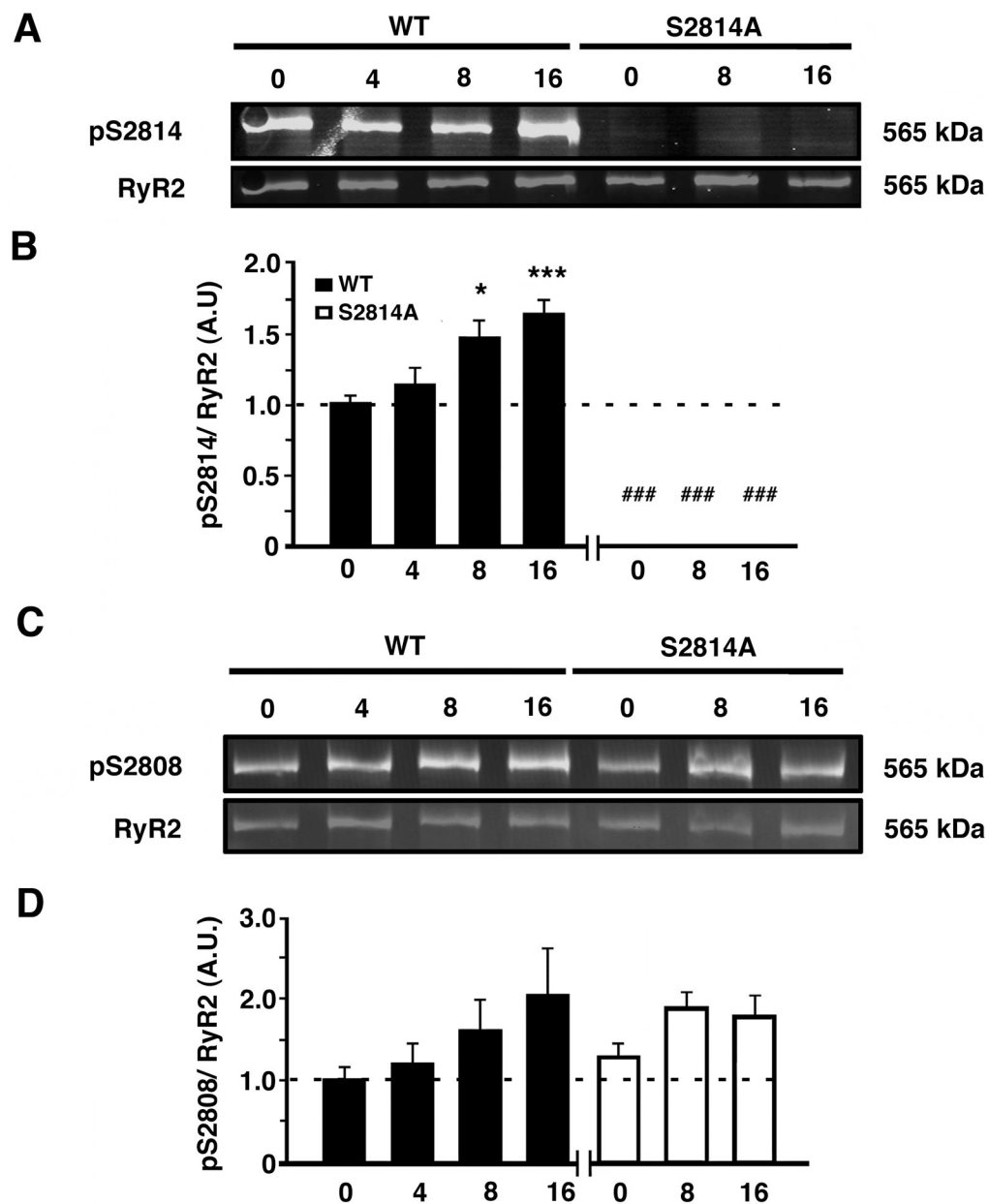


Figure 5. Increased CaMKII phosphorylation of RyR2 following TAC

A. Representative Western blots for phosphorylated RyR2-S2814 (pS2814) and total RyR2 in heart lysates from WT and S2814A mice before (0) or at 4, 8, and 16 weeks after TAC surgery, respectively. **B.** Quantification revealed increased S2814 phosphorylation starting at 8 weeks after TAC. Data (n=4–8 per group) represented as average \pm SEM. **C.** Representative Western blots for phosphorylated RyR2-S2808 (pS2808) and total RyR2 in heart lysates from WT and S2814A mice before (0) or at 4, 8, and 16 weeks after TAC surgery. **D.** Quantification showing non-significant increases in S2808 phosphorylation following TAC in WT and S2814A mice. Data (n=3–4 per group) represented as average \pm SEM. * $P < 0.05$ ** $P < 0.01$ versus corresponding sham, ### $P < 0.001$ versus WT TAC.

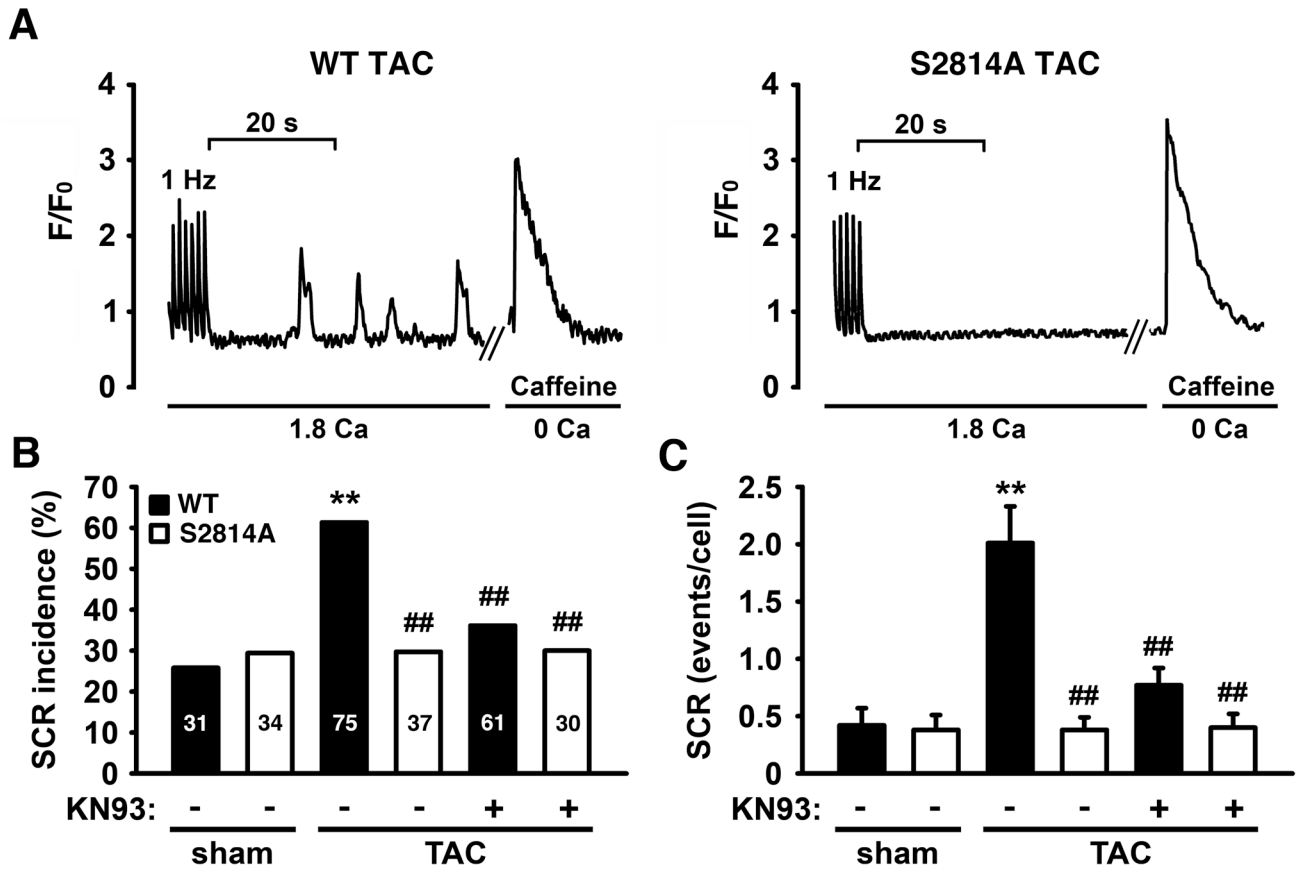


Figure 6. Inhibition of CaMKII phosphorylation of RyR2 attenuates SR Ca²⁺ Leak after TAC
A. Representative images of spontaneous Ca²⁺ release (SCR) events in ventricular myocytes after 1 Hz pacing. **B.** Incidence of SCR events in isolated myocytes from sham-operated and mice 16 weeks after TAC, before and after pre-treatment with KN93, respectively. **C.** Quantification of SCR events per cell before and after pre-treatment with KN93. N=30–75 cells from 3–6 mice per group. ** *P*<0.01 versus corresponding sham, ## *P*<0.01 versus WT TAC.

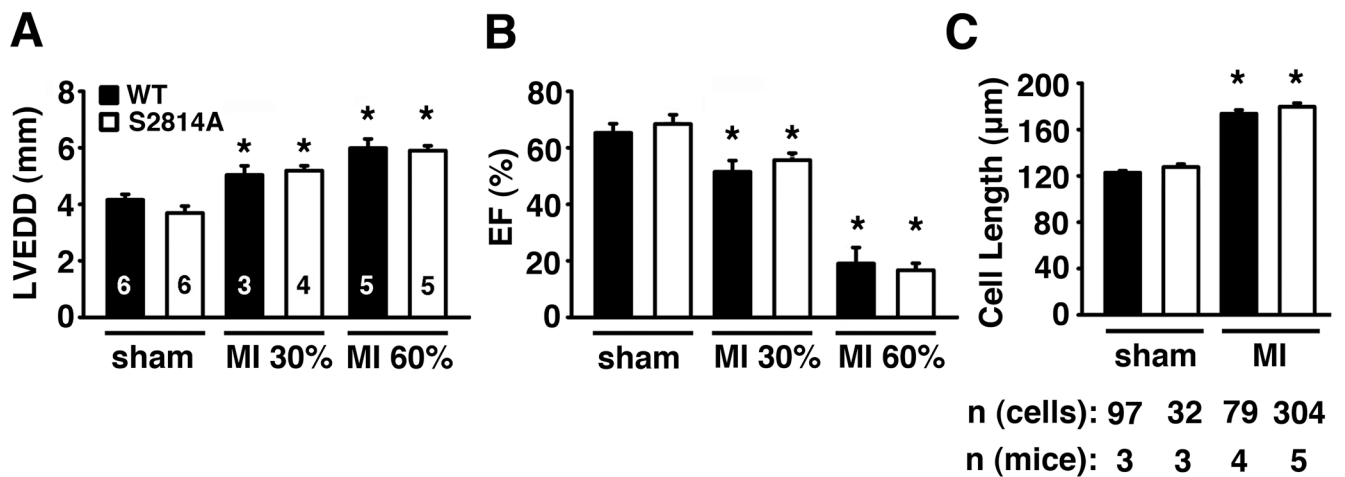


Figure 7. Inhibition of S2814 phosphorylation on RyR2 fails to protect against heart failure induced by MI

A, B. Echocardiographic analysis of WT and S2814A mice subjected to sham operation or myocardial infarction resulting in average infarcts comprising 30% or 60% of the left ventricle, respectively. There were no differences in left ventricular end-diastolic diameter (LVEDD) (**A**) or ejection fraction (EF) (**B**) comparing WT and S2814A. Numbers in bars indicate number of animals in panels A–B. **C.** Quantification of isolated ventricular myocyte length in WT and S2814A mice after MI. Numbers indicate number of animals and cells per group. * $P < 0.05$ versus corresponding sham.

Table 1

Echocardiographic parameters of WT and S2814A mice at 8 and 16 weeks after sham or TAC surgery.

	8 weeks				16 weeks			
	Sham		TAC		sham		TAC	
	WT (n=8)	S2814A (n=9)	WT (n=13)	S2814A (n=9)	WT (n=8)	S2814A (n=9)	WT (n=13)	S2814A (n=9)
HR (bpm)	462.1±10.5	467.9±16.1	489.2±12.3	471.3±16.0	477.4±8.8	448.9±14.4	481.1±12.5	475.0±14.9
ESD (mm)	2.76±0.08	2.75±0.07	3.36±0.14*	3.12±0.21	2.82±0.08	2.75±0.09	3.92±0.22***	3.25±0.16#
EDD (mm)	4.00±0.08	3.94±0.08	4.22±0.11	3.95±0.07	4.02±0.08	3.93±0.10	4.61±0.17*	4.10±0.13
EF (%)	59.2±1.5	58.0±1.0	42.1±2.6***	43.7±2.2***	57.7±1.3	57.9±1.1	32.5±3.4***	43.0±2.9***, #
FS (%)	31.1±1.0	30.2±0.7	20.7±1.4***	21.3±1.2***	30.0±0.9	30.1±0.7	15.5±1.7***	21.1±1.6***, #
IVSd (mm)	0.75±0.02	0.74±0.01	0.84±0.03	0.77±0.03	0.71±0.02	0.70±0.02	0.72±0.01	0.76±0.01*
IVSs (mm)	0.88±0.02	0.85±0.02	0.94±0.02	0.85±0.04	0.83±0.02	0.80±0.02	0.77±0.02	0.83±0.02
LVPWd (mm)	0.66±0.03	0.65±0.02	0.90±0.03***	0.84±0.04**	0.69±0.04	0.69±0.01	0.78±0.02	0.83±0.04*
LVPWs (mm)	0.95±0.03	0.95±0.03	1.11±0.03*	1.10±0.04*	0.97±0.04	0.99±0.02	0.94±0.02	1.07±0.04#

Data are expressed as mean ± SEM.

* $P<0.05$,

** $P<0.01$,

*** $P<0.001$ versus corresponding sham,

$P<0.05$ versus WT TAC. HR = heart rate; ESD = end-systolic diameter; EDD = end-diastolic diameter; EF = ejection fraction; FS = left ventricular fractional shortening; IVS = intraventricular septal wall thickness; LVPWd = left ventricular posterior wall thickness.